

Article

Fault-Tolerant Terminal Sliding Mode Control with Disturbance Observer for Vibration Suppression in Non-Local Strain Gradient Nano-Beams

Hajid Alsubaie ¹, Amin Yousefpour ^{2,*}, Ahmed Alotaibi ¹ , Naif D. Alotaibi ³ and Hadi Jahanshahi ⁴ ¹ Department of Mechanical Engineering, College of Engineering, Taif University, Taif 21944, Saudi Arabia² Department of Mechanical and Aerospace Engineering, University of California, Irvine, CA 92697, USA³ Communication Systems and Networks Research Group, Department of Electrical and Computer Engineering, Faculty of Engineering, King Abdulaziz University, Jeddah 21589, Saudi Arabia⁴ Department of Mechanical Engineering, University of Manitoba, Winnipeg, MB R3T 5V6, Canada

* Correspondence: yousefpo@uci.edu

Abstract: This research investigates the stabilization and control of an uncertain Euler–Bernoulli nano-beam with fixed ends. The governing partial differential equations of motion for the nano-beam are derived using Hamilton’s principle and the non-local strain gradient theory. The Galerkin method is then applied to transform the resulting dimensionless partial differential equation into a nonlinear ordinary differential equation. A novel fault-tolerant terminal sliding mode control technique is proposed to address the uncertainties inherent in micro/nano-systems and the potential for faults and failures in control actuators. The proposed controller includes a finite time estimator, the stability of which and the convergence of the error dynamics are established using the Lyapunov theorem. The significance of this study lies in its application to the field of micro/nano-mechanics, where the precise control and stabilization of small-scale systems is crucial for the development of advanced technologies such as nano-robotics and micro-electromechanical systems (MEMS). The proposed control technique addresses the inherent uncertainties and potential for faults in these systems, making it a valuable choice for practical applications. The simulation results are presented to demonstrate the effectiveness of the proposed control scheme and the high accuracy of the estimation algorithm.

Keywords: robust adaptive control; non-local strain gradient theory; fault-tolerant terminal sliding mode control; finite time disturbance observer; nonlinear vibrations; Hamiltonian principle

MSC: 93C40; 74H45; 74S40



Citation: Alsubaie, H.; Yousefpour, A.; Alotaibi, A.; Alotaibi, N.D.; Jahanshahi, H. Fault-Tolerant Terminal Sliding Mode Control with Disturbance Observer for Vibration Suppression in Non-Local Strain Gradient Nano-Beams. *Mathematics* **2023**, *11*, 789. <https://doi.org/10.3390/math11030789>

Academic Editor: António Lopes

Received: 29 December 2022

Revised: 23 January 2023

Accepted: 30 January 2023

Published: 3 February 2023



Copyright: © 2023 by the authors. Licensee MDPI, Basel, Switzerland. This article is an open access article distributed under the terms and conditions of the Creative Commons Attribution (CC BY) license (<https://creativecommons.org/licenses/by/4.0/>).

1. Introduction

Micro/nano-electromechanical systems (MEMS/NEMS) are miniaturized devices that operate at the micro/nanoscale and have a wide range of applications in various fields, including healthcare [1], electronics, the automotive industry, aerospace, and defense [2]. Micro/nano-beams are an important component of these systems because they can be used to transfer forces, displacements, and other mechanical quantities between different parts of the device. Some specific examples of the use of micro/nano-beams in MEMS/NEMS include:

- **Bio-MEMS [1]:** These are devices that use micro/nano-scale technology to interact with biological systems, such as cells, tissues, and organs. Micro/nano-beams can be used in bio-MEMS to create mechanical forces that stimulate or sense biological responses or to perform other functions such as drug delivery or tissue engineering.
- **Atomic force microscopes [3]:** These are advanced imaging tools that use a micro/nano-scale cantilever beam to probe the surface of a sample at a very high resolution. The

beam is used to sense the interaction forces between the sample and the tip of the beam, which can be used to create a detailed map of the sample's surface.

- Micro-switches [2]: These are tiny switches that can be used to control the flow of electrical current in a circuit. Micro/nano-beams can be used in micro-switches to actuate the switch and change the state of the circuit.
- Micro-actuators [4]: These are devices that can generate mechanical forces or displacements in response to an electrical or other input. Micro/nano-beams can be used as actuators in MEMS/NEMS to create small, precise movements.
- Micro-resonators [5]: These are devices that can vibrate at a specific frequency, and are used in a variety of applications including sensors, oscillators, and filters. Micro/nano-beams can be used to create the resonant motion in micro-resonators.
- Micro-sensors [6]: These are devices that can detect and measure physical quantities such as temperature, pressure, humidity, or chemical concentrations. Micro/nano-beams can be used in micro-sensors to sense these quantities and convert them into an electrical signal.

In addition to these examples, micro/nano-beams are also used in printers to improve the speed and quality of printing and to lower production costs and increase the number of dots per inch (dpi) [7]. Overall, micro/nano-beams are a versatile and essential component of many micro/nano-electromechanical systems, and they have the potential to revolutionize a wide range of fields and applications [8].

The mechanical and physical behavior of micro/nano-beams has been extensively studied through both experimental observations and theoretical methods [9,10].

To date, several studies have investigated various theories for modeling nano- and microsystems. These theories include continuum mechanics, molecular dynamics, and quantum mechanics, among others. Each theory has its own advantages and disadvantages, and the choice of which theory to use depends on the specific system being studied and the level of accuracy required. For example, continuum mechanics is widely used for modeling large-scale systems, while molecular dynamics and quantum mechanics are used for modeling small-scale systems at the atomic and subatomic level. Additionally, some theories have been developed specifically for nano and micro-systems, such as the non-local strain gradient theory, which takes into account the size-dependent behavior of these systems. Overall, there is a wide range of theories available for modeling nano- and micro-systems, and the choice of which theory to use should be made based on the specific characteristics and requirements of the system being studied [11].

Molecular dynamic (MD) simulation allows for the analysis of nano-structures at the atomic level [12]. However, this method can be time-consuming and may not be practical for all situations. On the other hand, the classical continuum mechanics theory, which is based on the study of large-scale materials, may not be accurate for the analysis of micro/nano-structures due to the lack of an additional length scale parameter and the importance of intermolecular forces on small scales. In addition, there are uncertainties about obtaining elasticity constants, such as the modulus of elasticity, using the discrete space model of micro/nano-structures with a continuum [13]. To address these issues, the non-classical continuum theory has become a popular choice for the analysis of micro/nano-structures. It offers the benefits of not requiring a long time for analysis and being more accurate than classical continuum theory [14]. Non-classical continuum theory includes various approaches, such as fractional calculus, which have been shown to be effective in the analysis of micro/nano-scale systems. In general, the use of non-classical continuum theory has become more prevalent in the analysis of micro/nano-structures due to its accuracy and efficiency compared to other methods [15].

One of the non-classical continuum theories developed for modeling size-dependent beams is the couple stress theory [16,17]. The strain gradient theory, which takes into account the strain energy being a function of the amount of strain and its first derivative [18], has been introduced in [19], and the modified strain gradient theory has been proposed in [20]. Similarly, the non-local elasticity theory [21] considers the stress at a point as a

function of strains at all points in the continuum, but only characterizes the softening effect and does not consider stiffness enhancement. However, strain gradient and couple stress theories can be used to incorporate stiffness enhancement. Therefore, the non-local elasticity theory, strain gradient theory, and couple stress theory address different aspects of size-dependent material behavior. Consequently, the combination of the non-local elasticity theory [15] and the strain gradient theory [22], called the non-local strain gradient theory [23], is essential for accurately modeling real size-dependent mechanical behavior.

The nonlinear control of MEMS/NEMS has been a subject of significant research in recent years due to the importance of these micro/nano-scale systems in a variety of applications. The small size and high sensitivity of these systems make them prone to nonlinear behavior, which can affect their performance and stability [24,25]. Therefore, developing effective control strategies for nonlinear MEMS/NEMS systems is essential for ensuring their reliable operation. One approach that has been widely used for nonlinear control of MEMS/NEMS is sliding mode control (SMC). SMC is a robust control method that can effectively handle uncertainties and perturbations in the system, making it well-suited for micro/nano-scale systems where these factors can have a significant impact on performance.

SMC works by driving the system to a sliding surface in the state space, where the control input is applied in such a way as to maintain the system on the surface [26–29]. This allows the system to track a desired reference signal while rejecting external disturbances and uncertainties. There have been many successful applications of SMC to the nonlinear control of MEMS/NEMS systems. For example, it has been used to control the vibration of micro-resonators, stabilize the nonlinear dynamics of micro/nano-beams, and improve the performance of micro/nano-actuators. In these applications, SMC has been shown to be an effective method for improving the accuracy and reliability of micro/nano-scale systems. In addition to these practical applications, there has also been significant research on the theoretical foundations of SMC for nonlinear MEMS/NEMS systems, including the development of new control laws and the study of stability and convergence properties. Overall, the use of SMC for nonlinear control of MEMS/NEMS has proven to be a valuable tool for improving the performance and reliability of these systems [30–33]. On the other hand, the existence of faults and failures in most of the practical systems is undeniable, and this makes considering their effects in the design of controller essential [34,35]. These issues demand more studies on the controller techniques for micro/nano-beams.

The precise control and stabilization of small-scale systems are essential for the development of advanced technologies such as nano-robotics and micro-electromechanical systems (MEMS). However, the inherent uncertainties and potential for faults in these systems pose significant challenges for control design. To address these challenges, the authors propose a novel fault-tolerant terminal sliding mode control technique. The proposed controller includes a finite time estimator, the stability of which and the convergence of the error dynamics are established using the Lyapunov theorem. The effectiveness of the proposed control scheme and the high accuracy of the estimation algorithm are demonstrated through the simulation results. This research is novel in its approach to addressing the specific challenges that arise in the control of micro/nano-systems, and it has the potential to greatly improve the precision and robustness of small-scale systems, ultimately leading to the development of advanced technologies such as nano-robotics and MEMS.

The paper is structured as follows: Section 2 introduces the mathematical model of a simply supported Euler–Bernoulli nano-beam subjected to a centralized force in the middle of the beam. Section 3 presents the design of the proposed controller. In Section 4, numerical simulations are presented to demonstrate the effectiveness and performance of the proposed control architecture and estimation algorithm for stabilizing the nonlinear vibration of the nano-beam. Finally, the conclusions are presented in Section 5.

2. System Model and Mathematical Formulation

The strain energy (U) of an isotropic linear elastic material can be described using the non-local strain gradient theory [23]:

$$U = \frac{1}{2} \int_V (\sigma_{xx}\varepsilon_{xx} + \sigma_{xx}^{(1)}\nabla\varepsilon_{xx})dV \tag{1}$$

where σ_{xx} , $\sigma_{xx}^{(1)}$, and ε_{xx} indicate the classical stress, the higher-order stress, and the normal strain, respectively. In addition, the one-dimensional differential operator is represented by ∇ in which is equal to $\partial/\partial x$. In addition, σ_{xx} and $\sigma_{xx}^{(1)}$ can be defined as

$$\sigma_{xx} = \int_0^L E\alpha_0(x, x', e_0a)\varepsilon'_{xx}(x')dx' \tag{2}$$

$$\sigma_{xx}^{(1)} = l_m^2 \int_0^L E\alpha_1(x, x', e_1a)\varepsilon'_{xx,x}(x')dx' \tag{3}$$

$$t_{xx} = \sigma_{xx} - \nabla\sigma_{xx}^{(1)} \tag{4}$$

where L , α_0 , α_1 , and E stand for the length of the nano-beam, the principal attenuation kernel function combining constitutive equations of the non-local effects, an additional kernel function relating to the non-local effect, and the Young’s modulus, respectively. In addition, the effects of the non-local elastic stress field are expressed by e_0a and e_1a . The strain gradient length scale parameter is represented by l_m . The general non-local strain gradient constitutive equation is given by [23]:

$$[1 - (e_0a)^2\nabla^2][1 - (e_1a)^2\nabla^2]t_{xx} = E[1 - (e_1a)^2\nabla^2]\varepsilon_{xx} - El_m^2[1 - (e_0a)^2\nabla^2]\nabla^2\varepsilon_{xx} \tag{5}$$

where $\nabla^2 = \frac{\partial^2}{\partial x^2}$ is the Laplacian operator. Let $e_0 = e_1 = e$ [23] and Equation (5) can be rewritten as

$$[1 - (ea)^2\nabla^2]t_{xx} = E(1 - l_m^2\nabla^2)\varepsilon_{xx} \tag{6}$$

Supposing $l_m = 0$ results in non-local elasticity theory as [21]:

$$[1 - (ea)^2\nabla^2]t_{xx} = E\varepsilon_{xx} \tag{7}$$

In addition, considering $ea = 0$, the strain gradient theory is given by [22]

$$t_{xx} = E(1 - l_m^2\nabla^2)\varepsilon_{xx} \tag{8}$$

The structure of a hinged–hinged nano-beams is illustrated in Figure 1.

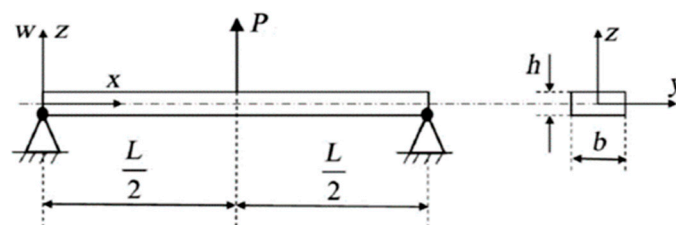


Figure 1. A hinged-hinged nano-beam.

Considering Figure 1, the displacement components of a straight Euler–Bernoulli nano-beam can be represented as:

$$\begin{aligned} u_1(x, z, t) &= u(x, t) - z\frac{\partial w(x, t)}{\partial x} \\ u_2(x, z, t) &= 0 \\ u_3(x, z, t) &= w(x, t) \end{aligned} \tag{9}$$

The displacements in the $x, y,$ and z directions are represented by $u_1, u_2,$ and $u_3,$ respectively. When considering large deflection and small slope for a straight Euler–Bernoulli nano-beam, Von Karman’s nonlinear strain relationship can be expressed as follows:

$$\epsilon_{xx} = \frac{\partial u(x,t)}{\partial x} + \frac{1}{2} \left(\frac{\partial w(x,t)}{\partial x} \right)^2 - z \frac{\partial^2 w(x,t)}{\partial x^2} \tag{10}$$

in which ϵ_{xx} denotes the longitudinal strain. The first variation of strain energy is given by:

$$\delta \int_0^t U dt = \int_0^t \int_V \left(\sigma_{xx} \delta \epsilon_{xx} + \sigma_{xx}^{(1)} \nabla \delta \epsilon_{xx} \right) dV dt \tag{11}$$

Equation (11) can be rewritten as follows:

$$\begin{aligned} \delta \int_0^t U dt &= \int_0^t \int_V \left(\sigma_{xx} \delta \epsilon_{xx} - \nabla \sigma_{xx}^{(1)} \delta \epsilon_{xx} \right) dV dt + \int_0^t \left[\int_A \sigma_{xx}^{(1)} \delta \epsilon_{xx} dA \right]_0^L dt \\ &= \int_0^t \int_V (t_{xx} \delta \epsilon_{xx}) dV dt + \int_0^t \left[\int_A \sigma_{xx}^{(1)} \delta \epsilon_{xx} dA \right]_0^L dt \end{aligned} \tag{12}$$

where A is the cross-sectional area. Now, we define the following stress resultants as:

$$N_c = \int_A t_{xx} dA, M_c = \int_A z t_{xx} dA, N_{nc} = \int_A \sigma_{xx}^{(1)} dA, M_{nc} = \int_A z \sigma_{xx}^{(1)} dA \tag{13}$$

where M_c and N_c are the classical normal moment and force, respectively; in addition, M_{nc} and N_{nc} indicate the non-classical ones. Substituting Equations (10) and (13) into Equation (12) results in:

$$\begin{aligned} \delta \int_0^t U dt &= \int_0^t \int_0^L \left[N_c \left(\frac{\partial \delta u}{\partial x} + \frac{\partial w}{\partial x} \frac{\partial \delta w}{\partial x} \right) - M_c \frac{\partial^2 \delta w}{\partial x^2} \right] dx dt \\ &+ \int_0^t \left[N_{nc} \left(\frac{\partial \delta u}{\partial x} + \frac{\partial w}{\partial x} \frac{\partial \delta w}{\partial x} \right) - M_{nc} \frac{\partial^2 \delta w}{\partial x^2} \right]_0^L dt \end{aligned} \tag{14}$$

In addition, for the work that is carried out by the applied external forces, one has:

$$\delta \int_0^t W dt = \int_0^t \int_L (f \delta u + q \delta w) dx dt \tag{15}$$

where f and q represent the distributed axial and transverse loads, respectively. Similarly, the first variation of kinetic energy is given by:

$$\delta \int_0^t K_e dt = \int_0^t \int_0^L I_A \left(\frac{\partial u}{\partial t} \frac{\partial \delta u}{\partial t} + \frac{\partial w}{\partial t} \frac{\partial \delta w}{\partial t} \right) dx dt \tag{16}$$

where

$$I_A = \frac{1}{12} b h^3 \tag{17}$$

The general form of Hamilton’s principle, which is used to derive the equations of motion, is as follows:

$$\delta \int_0^t [K_e - (U - W)] dt = 0 \tag{18}$$

By applying Hamilton’s principle (18) and separating the coefficients of δu and $\delta w,$ the governing equation of the system can be reached as follows:

$$\begin{aligned} \delta u &\Rightarrow \frac{\partial N_c}{\partial x} + f(x,t) = I_A \frac{\partial^2 u}{\partial t^2} \\ \delta w &\Rightarrow \frac{\partial^2 M_c}{\partial x^2} + \frac{\partial}{\partial x} \left(N_c \frac{\partial w}{\partial x} \right) + q(x,t) = I_A \frac{\partial^2 w}{\partial t^2} \end{aligned} \tag{19}$$

Moreover, the corresponding boundary conditions are:

$$\begin{aligned}
 \delta u &\Rightarrow N_c = 0 \text{ or } u = 0 \\
 \frac{\delta \delta u}{\delta x} &\Rightarrow N_{nc} = 0 \text{ or } \frac{\partial u}{\partial x} = 0 \\
 \delta w &\Rightarrow \frac{\partial M_c}{\partial x} + N_c \frac{\partial w}{\partial x} = 0 \text{ or } w = 0 \\
 \frac{\delta \delta w}{\delta x} &\Rightarrow M_c - N_{nc} \frac{\partial w}{\partial x} = 0 \text{ or } \frac{\partial w}{\partial x} = 0 \\
 \frac{\delta \delta^2 w}{\delta x^2} &\Rightarrow M_{nc} = 0 \text{ or } \frac{\partial^2 w}{\partial x^2} = 0
 \end{aligned}
 \tag{20}$$

Equation (6) can be modified to apply to a nano-beam using the non-local strain gradient theory as follows:

$$\begin{aligned}
 t_{xx} - (ea)^2 \frac{\partial^2 t_{xx}}{\partial x^2} &= E \left[\frac{\partial u}{\partial x} + \frac{1}{2} \left(\frac{\partial w}{\partial x} \right)^2 - z \frac{\partial^2 w}{\partial x^2} \right] \\
 &\quad - El_m^2 \left[\frac{\partial^3 u}{\partial x^3} + \frac{\partial w}{\partial x} \frac{\partial^3 w}{\partial x^3} + \left(\frac{\partial^2 w}{\partial x^2} \right)^2 - z \frac{\partial^4 w}{\partial x^4} \right]
 \end{aligned}
 \tag{21}$$

According to Equations (13) and (21), one has:

$$\begin{aligned}
 N_c - (ea)^2 \frac{\partial^2 N_c}{\partial x^2} &= A_{xx} \left[\frac{\partial u}{\partial x} + \frac{1}{2} \left(\frac{\partial w}{\partial x} \right)^2 \right] - A_{xx} l_m^2 \left[\frac{\partial^3 u}{\partial x^3} + \frac{\partial w}{\partial x} \frac{\partial^3 w}{\partial x^3} + \left(\frac{\partial^2 w}{\partial x^2} \right)^2 \right] \\
 M_c - (ea)^2 \frac{\partial^2 M_c}{\partial x^2} &= -D_{xx} \frac{\partial^2 w}{\partial x^2} + D_{xx} l_m^2 \frac{\partial^4 w}{\partial x^4}
 \end{aligned}
 \tag{22}$$

where

$$(A_{xx}, D_{xx}) = \int_A E (1, z^2) dA, B_{xx} = \int_A E z dA = 0
 \tag{23}$$

Now, based on Equation (19), we substitute $\frac{\partial N_c}{\partial x}$ and $\frac{\partial^2 M_c}{\partial x^2}$ into Equation (22), which yields:

$$\begin{aligned}
 N_c &= A_{xx} \left[\frac{\partial u}{\partial x} + \frac{1}{2} \left(\frac{\partial w}{\partial x} \right)^2 \right] - A_{xx} l_m^2 \left[\frac{\partial^3 u}{\partial x^3} + \frac{\partial w}{\partial x} \frac{\partial^3 w}{\partial x^3} + \left(\frac{\partial^2 w}{\partial x^2} \right)^2 \right] + (ea)^2 \left(I_A \frac{\partial^3 u}{\partial x^3} - \frac{\partial f}{\partial x} \right) \\
 M_c &= -D_{xx} \frac{\partial^2 w}{\partial x^2} + D_{xx} l_m^2 \frac{\partial^4 w}{\partial x^4} + (ea)^2 \left[I_A \frac{\partial^2 w}{\partial x^2} - \frac{\partial}{\partial x} \left(N_c \frac{\partial w}{\partial x} \right) - q \right]
 \end{aligned}
 \tag{24}$$

Substituting Equation (19) in Equation (24) yields:

$$\begin{aligned}
 &\frac{\partial}{\partial x} \left\{ \left[A_{xx} \frac{\partial u}{\partial x} + \frac{A_{xx}}{2} \left(\frac{\partial w}{\partial x} \right)^2 \right] - \left[A_{xx} l_m^2 \frac{\partial^3 u}{\partial x^3} + A_{xx} l_m^2 \left(\frac{\partial w}{\partial x} \frac{\partial^3 w}{\partial x^3} + \left(\frac{\partial^2 w}{\partial x^2} \right)^2 \right) \right] \right\} \\
 &+ I_A \frac{\partial^2}{\partial x^2} \left[(ea)^2 \frac{\partial^2 u}{\partial x^2} - u \right] = (ea)^2 \frac{\partial^2 f}{\partial x^2} - f \\
 &D_{xx} l_m^2 \frac{\partial^6 w}{\partial x^6} - D_{xx} \frac{\partial^4 w}{\partial x^4} + \frac{\partial}{\partial x} \left(N_c \frac{\partial w}{\partial x} \right) - (ea)^2 \frac{\partial^3}{\partial x^3} \left(N_c \frac{\partial w}{\partial x} \right) \\
 &+ I_A \frac{\partial^2}{\partial x^2} \left[(ea)^2 \frac{\partial^2 w}{\partial x^2} - w \right] = (ea)^2 \frac{\partial^2 q}{\partial x^2} - q
 \end{aligned}
 \tag{25}$$

If we assume that the rotational inertia of the beam is negligible, the governing equation of the system, which is a function of u and its derivatives, can be written as follows:

$$\frac{\partial}{\partial x} \left\{ \left[A_{xx} \frac{\partial u}{\partial x} + \frac{A_{xx}}{2} \left(\frac{\partial w}{\partial x} \right)^2 \right] - \left[A_{xx} l_m^2 \frac{\partial^3 u}{\partial x^3} + A_{xx} l_m^2 \left(\frac{\partial w}{\partial x} \frac{\partial^3 w}{\partial x^3} + \left(\frac{\partial^2 w}{\partial x^2} \right)^2 \right) \right] \right\} = \frac{\partial}{\partial x} (N_c) = 0
 \tag{26}$$

According to Equation (26), it can be concluded that N_c remains unchanged. By integrating both sides of equation (26), we obtain the following equation:

$$\frac{\partial u}{\partial x} + \frac{1}{2} \left(\frac{\partial w}{\partial x} \right)^2 - l_m^2 \frac{\partial^3 u}{\partial x^3} - l_m^2 \left(\frac{\partial w}{\partial x} \frac{\partial^3 w}{\partial x^3} + \left(\frac{\partial^2 w}{\partial x^2} \right)^2 \right) = \frac{C}{A_{xx}}
 \tag{27}$$

where C is a constant parameter. The boundary condition for the hinged–hinged beam is:

$$u(0, t) = u(L, t) = \frac{\partial^2 u(0, t)}{\partial x^2} = \frac{\partial^2 u(L, t)}{\partial x^2} = 0
 \tag{28}$$

By using the strain gradient theory [22], as described in Equation (28), applying the boundary conditions related to the second derivatives and integrating both sides of Equation (27) over the length of the beam (from $x = 0$ to $x = L$), we can derive the following equation:

$$\frac{CL}{A_{xx}} = [u(L, t) - u(0, t)] - l_m^2 \left[\frac{\partial^2 u(L, t)}{\partial x^2} - \frac{\partial^2 u(0, t)}{\partial x^2} \right] + \frac{1}{2} \int_0^L \left(\frac{\partial w}{\partial x} \right)^2 dx - l_m^2 \int_0^L \left(\frac{\partial w}{\partial x} \frac{\partial^3 w}{\partial x^3} + \left(\frac{\partial^2 w}{\partial x^2} \right)^2 \right) dx \tag{29}$$

Hence

$$\frac{CL}{A_{xx}} = [u(L, t) - u(0, t)] - l_m^2 \left[\frac{\partial^2 u(L, t)}{\partial x^2} - \frac{\partial^2 u(0, t)}{\partial x^2} \right] + \frac{1}{2} \int_0^L \left(\frac{\partial w}{\partial x} \right)^2 dx - l_m^2 \int_0^L \left(\frac{\partial w}{\partial x} \frac{\partial^3 w}{\partial x^3} + \left(\frac{\partial^2 w}{\partial x^2} \right)^2 \right) dx \tag{30}$$

$$N_c = \frac{A_{xx}}{2L} \int_0^L \left(\frac{\partial w}{\partial x} \right)^2 dx - \frac{A_{xx} l_m^2}{L} \int_0^L \left(\frac{\partial w}{\partial x} \frac{\partial^3 w}{\partial x^3} + \left(\frac{\partial^2 w}{\partial x^2} \right)^2 \right) dx \tag{31}$$

Substituting Equation (31) into Equation (25) results in the governing equation for the nano-beam based on the nonlocal strain gradient theory, which is expressed as follows [15]:

$$D_{xx} l_m^2 \frac{\partial^6 w}{\partial x^6} - D_{xx} \frac{\partial^4 w}{\partial x^4} + \left[\frac{A_{xx}}{2L} \int_0^L \left(\frac{\partial w}{\partial x} \right)^2 dx - \frac{A_{xx} l_m^2}{L} \int_0^L \left(\frac{\partial w}{\partial x} \frac{\partial^3 w}{\partial x^3} + \left(\frac{\partial^2 w}{\partial x^2} \right)^2 \right) dx \right] \times \left[\frac{\partial^2 w}{\partial x^2} - (ea)^2 \frac{\partial^4 w}{\partial x^4} \right] + I_A \frac{\partial^2}{\partial t^2} \left[(ea)^2 \frac{\partial^2 w}{\partial x^2} - w \right] = (ea)^2 \frac{\partial^2 q}{\partial x^2} - q \tag{32}$$

To express Equation (32) in dimensionless form, the following quantities are introduced:

$$\bar{x} = \frac{x}{L}, \bar{w} = \frac{w}{r}, \bar{z} = \frac{z}{h}, \bar{t} = t \sqrt{\frac{EI}{\rho AL^4}}, \alpha = \frac{ea}{L}, \beta = \frac{l_m}{L} \tag{33}$$

where $r = \sqrt{\frac{I}{A}}$. Therefore, the dimensionless governing equation is obtained as:

$$\beta^2 \bar{D}_{xx} \frac{\partial^6 \bar{w}}{\partial \bar{x}^6} - \bar{D}_{xx} \frac{\partial^4 \bar{w}}{\partial \bar{x}^4} + \left[\frac{\bar{A}_{xx}}{2} \int_0^1 \left(\frac{\partial \bar{w}}{\partial \bar{x}} \right)^2 d\bar{x} - \beta^2 \bar{A}_{xx} \int_0^1 \left(\frac{\partial \bar{w}}{\partial \bar{x}} \frac{\partial^3 \bar{w}}{\partial \bar{x}^3} + \left(\frac{\partial^2 \bar{w}}{\partial \bar{x}^2} \right)^2 \right) d\bar{x} \right] \frac{\partial^2 \bar{w}}{\partial \bar{x}^2} - \left[\frac{\alpha^2 \bar{A}_{xx}}{2} \int_0^1 \left(\frac{\partial \bar{w}}{\partial \bar{x}} \right)^2 d\bar{x} - \alpha^2 \beta^2 \bar{A}_{xx} \int_0^1 \left(\frac{\partial \bar{w}}{\partial \bar{x}} \frac{\partial^3 \bar{w}}{\partial \bar{x}^3} + \left(\frac{\partial^2 \bar{w}}{\partial \bar{x}^2} \right)^2 \right) d\bar{x} \right] \frac{\partial^4 \bar{w}}{\partial \bar{x}^4} + \alpha^2 \bar{I}_A \frac{\partial^4 \bar{w}}{\partial \bar{x}^2 \partial \bar{t}^2} - \bar{I}_A \frac{\partial^2 \bar{w}}{\partial \bar{t}^2} = \alpha^2 \frac{\partial^2 \bar{q}}{\partial \bar{x}^2} - \bar{q} \tag{34}$$

where

$$\bar{A}_{xx} = 1, \bar{D}_{xx} = 1, \bar{I}_A = 1 \tag{35}$$

In this study, we use the Galerkin approach to transform the partial differential equation into a nonlinear ordinary differential equation. To do this, we decompose the temporal and spatial terms of $\bar{w}(\bar{x}, \bar{t})$ as follows [36]:

$$\bar{w}(\bar{x}, \bar{t}) = Q(\bar{t})\phi(\bar{x}) \tag{36}$$

$$\phi(\bar{x}) = \sin(\pi\bar{x})$$

where $Q(\bar{t})$ represents the unknown temporal component that needs to be determined, while $\phi(\bar{x})$ represents the spatial component of the transverse deflection that satisfies the boundary conditions of the hinged-hinged nano-beam.

In addition, the concentrated force $\bar{q}(\bar{x}, \bar{t})$ is given by:

$$\bar{q}(\bar{x}, \bar{t}) = q(\bar{t})\delta\left(\bar{x} - \frac{1}{2}\right) \tag{37}$$

$$\int_{a-\epsilon}^{a+\epsilon} f(x)\delta(x-a)dx = f(a), \int_{a-\epsilon}^{a+\epsilon} f(x)\delta^{(n)}(x-a)dx = -\int_{a-\epsilon}^{a+\epsilon} \frac{\partial f}{\partial x} \delta^{(n-1)}(x-a)dx$$

Substituting Equations (36) and (37) in Equation (34), multiplying both sides of Equation (34) by $\phi(\bar{x})$, and by calculating the integral over the length of the beam, the ordinary differential equation (ODE) will be obtained as follows:

$$\ddot{Q}(\bar{t}) + K_1 Q(\bar{t}) + K_2 Q^3(\bar{t}) = -(\alpha^2 \pi^2 + 1)q(\bar{t}) \tag{38}$$

where the dot denotes the derivative with respect to time, and coefficients K_1 and K_2 are given by:

$$K_1 = \frac{\beta^2 \bar{D}_{xx} \int_0^1 \phi^{(6)} \phi d\bar{x} - \bar{D}_{xx} \int_0^1 \phi^{(4)} \phi d\bar{x}}{\alpha^2 \int_0^1 \phi'' \phi d\bar{x} - \int_0^1 (\phi')^2 d\bar{x}} \tag{39}$$

$$K_2 = -\frac{\frac{\bar{A}_{xx}}{2} \int_0^1 (\phi')^2 d\bar{x} \cdot \int_0^1 \phi'' \phi d\bar{x} - \beta^2 \bar{A}_{xx} \int_0^1 \phi''' \phi' d\bar{x} \cdot \int_0^1 \phi'' \phi d\bar{x} - \beta^2 \bar{A}_{xx} \int_0^1 (\phi'')^2 d\bar{x} \cdot \int_0^1 \phi'' \phi d\bar{x}}{\alpha^2 \int_0^1 \phi'' \phi d\bar{x} - \int_0^1 (\phi')^2 d\bar{x}} - \frac{\frac{\alpha^2 \bar{A}_{xx}}{2} \int_0^1 (\phi')^2 d\bar{x} \cdot \int_0^1 \phi^{(4)} \phi d\bar{x} - \alpha^2 \beta^2 \bar{A}_{xx} \int_0^1 \phi''' \phi' d\bar{x} \cdot \int_0^1 \phi^{(4)} \phi d\bar{x} - \alpha^2 \beta^2 \bar{A}_{xx} \int_0^1 (\phi'')^2 d\bar{x} \cdot \int_0^1 \phi^{(4)} \phi d\bar{x}}{\alpha^2 \int_0^1 \phi'' \phi d\bar{x} - \int_0^1 (\phi')^2 d\bar{x}} \tag{40}$$

where $\phi^{(4)}$ and $\phi^{(6)}$ are the fourth and sixth derivatives of ϕ with respect to time, respectively, and ϕ' is its first derivative with respect to \bar{x} . The state-space equation of the system is:

$$\begin{cases} Q(\bar{t}) = x_1, \dot{Q}(\bar{t}) = \dot{x}_1 = x_2 \\ \dot{x}_1 = x_2 \\ \dot{x}_2 = -K_1 x_1 - K_2 (x_1)^3 - bq(\bar{t}) \end{cases} \tag{41}$$

3. Controller Design

3.1. Problem Formulation

The non-local strain gradient nano-beams' general state space in the presence of disturbance is described using the following form:

$$\begin{cases} \dot{x}_i = x_{i+1} & i = 1, 2, \dots, n - 1 \\ \dot{x}_n = f(x) + g(x)u + d(t) \\ y = x_1 \end{cases} \tag{42}$$

where x_i and x_n stand for the states of the system. It is noteworthy that here we design the controller for general cases in which n could be any number, and for the nano-beam $n = 2$. $f(x)$ and $g(x)$ are nonlinear functions that describe the system dynamics. u represents the external control input, and $d(t)$ represents the disturbance.

According to the definitions of faults and failures presented in many sources, including [37–39], faults and/or failures are modelled as follows:

$$u = u_c + b(t)((e_i - 1)u_c + \bar{u}) \tag{43}$$

where u is the actual control input; u_c indicates the desired control input; and \bar{u} denotes the uncertain constant fault input. Parameter $0 \leq e_i \leq 1$ is considered to be the actuator control effectiveness. The time profile of a fault affecting the actuator is represented by time-varying function $b_i(t)$ which is given by:

$$b(t) = \begin{cases} 0, & t < t_0 \\ 1 - e_i^{-a_i(t-t_0)}, & t \geq t_0 \end{cases} \tag{44}$$

In this equation, $a_i > 0$ represents the unknown fault evolution rate, and t_i is the time of occurrence of the fault. An incipient fault occurs when a_i is small, while an abrupt fault occurs when a_i is large. The state space equation of the system in the presence of actuator faults and/or failures is given by:

$$\begin{cases} \dot{x}_i = x_{i+1} \quad i = 1, 2, \dots, n - 1 \\ \dot{x}_n = f(x) + g(x)u + N(t) \\ y = x_1 \\ N = g(x)b(t)((e_i - 1)u_c + \bar{u}) + d(t) \end{cases} \quad (45)$$

Assumption 1. *Uncertainties and disturbances are bounded, meaning there is a constant d_0 such that the norm of d is less than or equal to d_0 ($\|d\| \leq d_0$).*

Assumption 1 states that uncertainties and disturbances in the system are bounded, meaning there is a maximum limit on the magnitude of these disturbances, represented by a constant d_0 . This assumption can be mechanically motivated by the fact that in physical systems, disturbances and uncertainties are often caused by external factors such as environmental conditions, which are limited in their magnitude. For example, wind gusts or vibrations from nearby sources will have a maximum limit in terms of the forces they exert on the system.

Assumption 2. *Due to the physical limitations on the actuators, control actions are constrained, i.e., $|u_c| \leq u_{max}$. In addition, the additive fault \bar{u} is bounded, i.e., $|\bar{u}| \leq u_0$.*

Assumption 2 states that control actions are constrained due to the physical limitations of the actuators, meaning there is a maximum limit on the magnitude of the control inputs, represented by a constant u_{max} . Additionally, the assumption states that any additive fault in the system, represented by \bar{u} , is also bounded with a maximum limit of u_0 . This assumption can be mechanically motivated by the fact that actuators, such as motors and servos, have physical limitations on the amount of torque or force they can produce. Additionally, any additive faults in the system, such as sensor or actuator failures, will also have a maximum limit in terms of the impact they have on the system.

3.2. Finite-Time Disturbance-Observer-Based

To demonstrate the finite-time convergence of the closed-loop system and the error of the disturbance observer, Lemma 1 was utilized.

Lemma 1 [40]. *Let Lyapunov function $V(t)$ which fulfils the following inequality:*

$$\dot{V}(t) + \vartheta V(t) + \xi V^\chi \leq 0, \forall t > t_0 \quad (46)$$

The system will reach its equilibrium point in a finite time, as indicated by the following convergence time:

$$t_s \leq t_0 + \frac{1}{\vartheta(1 + \chi)} \ln \frac{\vartheta V^{1-\chi}(t_0) + \xi}{\xi} \quad (47)$$

where $\vartheta > 0, \xi > 0$ and $0 < \chi < 1$.

In the design process for the finite time estimator, the following auxiliary variables are defined:

$$s = z - x_n \quad (48)$$

where z is calculated by the following formula:

$$\dot{z} = -ks - \beta \text{sign}(s) - \varepsilon s^{p_0/q_0} - |f(x)| \text{sign}(s) + g(x)u \quad (49)$$

where $p_0 < q_0$ and q_0 and p_0 are odd positive integers. In addition, parameters k, ε , and β are positive and $\beta > |N|$. The disturbance estimation \hat{N} is given by:

$$\hat{N} = -ks - \beta \text{sign}(s) - \varepsilon s^{p_0/q_0} - |f(x)| \text{sign}(s) - f(x) \quad (50)$$

Considering Equations (46), (49) and (50) yields:

$$\dot{s} = \dot{z} - \dot{x}_n = -ks - \beta \text{sign}(s) - \varepsilon s^{p_0/q_0} - |f(x)| \text{sign}(s) - f(x) - N \tag{51}$$

Considering Equations (49)–(51), the following is achieved:

$$\begin{aligned} \tilde{N} &= \hat{N} - N = -ks - \beta \text{sign}(s) - \varepsilon s^{p_0/q_0} - |f(x)| \text{sign}(s) - f(x) - N \\ &= -ks - \beta \text{sign}(s) - \varepsilon s^{p_0/q_0} - |f(x)| \text{sign}(s) - f(x) - \dot{x}_n + f(x) + g(x)u \\ &= -ks - \beta \text{sign}(s) - \varepsilon s^{p_0/q_0} - |f(x)| \text{sign}(s) + g(x)u - \dot{x}_n \\ &= \dot{z} - \dot{x}_n = \dot{s} \end{aligned} \tag{52}$$

Theorem 1. *The disturbance estimator (49)–(51) ensures that the error of disturbance estimation converges to zero in finite time.*

Proof. Consider a Lyapunov function of the form:

$$V_0 = \frac{1}{2}s^2 \tag{53}$$

The time derivative of the Lyapunov function is given by:

$$\begin{aligned} \dot{V}_0 &= s\dot{s} = s(-ks - \beta \text{sign}(s) - \varepsilon s^{p_0/q_0} - |f(x)| \text{sign}(s) - f(x) - N) \\ &\leq -ks^2 - \beta s \text{sign}(s) - \varepsilon s^{p_0+q_0/q_0} + |s||N| \\ &\leq -ks^2 - \varepsilon s^{p_0+q_0/q_0} \\ &\leq -2kV_0 - 2^{(p_0+q_0)/2q_0} \varepsilon V_0^{(p_0+q_0)/2q_0} \end{aligned} \tag{54}$$

□

Considering Lemma 1 and Equation (54), it can be confirmed that in the finite time, the auxiliary variable s and, as a result, the disturbance estimation error converge to zero.

Herein, to design the fault-tolerant terminal sliding mode controller, the following sliding surfaces are defined:

$$\begin{aligned} s_1 &= y - y_d \\ s_1^{(n)} &= y^{(n)} - y_d^{(n)} = \dot{x}_n - y_d^{(n)}, \end{aligned} \tag{55}$$

We use the following recursive procedure to design n th sliding surface:

$$\begin{aligned} s_2 &= \dot{s}_1 + \alpha_1 s_1 + \beta_1 s_1^{p_1/q_1} \\ s_3 &= \dot{s}_2 + \alpha_2 s_2 + \beta_2 s_2^{p_2/q_2} \\ &\dots \\ s_n &= \dot{s}_{n-1} + \alpha_{n-1} s_{n-1} + \beta_{n-1} s_{n-1}^{p_{n-1}/q_{n-1}} + s \end{aligned} \tag{56}$$

The j th-order time derivative of s_i is calculated as follows:

$$s_i^{(j)} = s_{i-1}^{(i+1)} + \frac{d^{(j)}}{dt^{(j)}} \left[\alpha_{i-1} s_{i-1} + \beta_{i-1} s_{i-1}^{p_{i-1}/q_{i-1}} \right] \tag{57}$$

On the basis of Equations (56) and (57), the following equation is obtained:

$$\dot{s}_n = s_1^{(n)} + \sum_{j=1}^{n-1} \alpha_j s_j^{(n-j)} + \sum_{j=1}^{n-1} \beta_j \frac{d^{(n-j)}}{dt^{(n-j)}} s_j^{p_j/q_j} + \dot{s} \tag{58}$$

In accordance with Equations (45), (55) and (58) we have:

$$\begin{aligned} \dot{s}_n &= \dot{x}_n - \dot{y}_d^{(n)} + \sum_{j=1}^{n-1} \alpha_j s_j^{(n-j)} + \sum_{j=1}^{n-1} \beta_j \frac{d^{(n-j)}}{dt^{(n-j)}} s_j^{p_j/q_j} + \dot{s} \\ &= f(x) + g(x)u + d - \dot{y}_d^{(n)} + \sum_{j=1}^{n-1} \alpha_j s_j^{(n-j)} + \sum_{j=1}^{n-1} \beta_j \frac{d^{(n-j)}}{dt^{(n-j)}} s_j^{p_j/q_j} + \dot{s} \end{aligned} \tag{59}$$

Finally, the disturbance-observer-based fault-tolerant tracking control law is given by:

$$\begin{aligned} u &= -\frac{u_0}{g(x)} \\ u_0 &= f(x) - \dot{y}_d^{(n)} + \sum_{j=1}^{n-1} \alpha_j s_j^{(n-j)} + \sum_{j=1}^{n-1} \beta_j \frac{d^{(n-j)}}{dt^{(n-j)}} s_j^{p_j/q_j} + \hat{N} + \delta s_n + \mu s_n^{p_n/q_n} \end{aligned} \tag{60}$$

where user-defined parameters δ and μ should be positive.

Theorem 2. *The proposed control law (60) ensures that the states of the system (43) will converge to the desired value in finite time, even in the presence of uncertainties, external disturbances, and faults in the control actuators.*

Proof. Substituting Equation (61) into Equation (60) yields:

$$\dot{s}_2 = -\delta s_2 - \mu s_2^{p_2/q_2} + N - \hat{N} + \dot{s} = -\delta s_2 - \mu s_2^{p_2/q_2} - \tilde{N} + \dot{s} \tag{61}$$

In accordance with Equation (52), we know that after finite time $\tilde{N} = \dot{s}$; thus, we obtain:

$$\dot{s}_2 = -\delta s_2 - \mu s_2^{p_2/q_2} \tag{62}$$

Now, assume a Lyapunov function candidate as:

$$V = \frac{1}{2} s_2^2 \tag{63}$$

the time derivative of V is given by:

$$\begin{aligned} \dot{V} &= s_2 \dot{s}_2 = -\delta s_2^2 - \mu s_2^{1+(\frac{p_2}{q_2})} \\ &= -2\delta V - \mu 2^{(p_2+q_2)/2q_2} V^{(p_2+q_2)/2q_2} \end{aligned} \tag{64}$$

□

Based on Lemma 1 and Equation (64), the states of the closed-loop system will converge to the equilibrium point in finite time, which completes the proof.

The block diagram of the proposed control technique is shown by Figure 2. Based on Equation (60), the disturbances, as well as faults and failures, were considered in the model, and it makes the designed controller an appropriate and robust choice for the control of nano-beams.

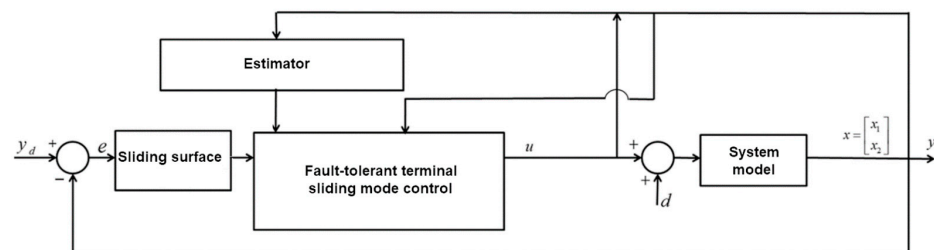


Figure 2. Block diagram of disturbance-observer-based fault-tolerant terminal sliding mode control for vibration suppression of non-local strain gradient nano-beams.

4. Numerical Simulations

In this section, the numerical simulation for the stabilization of the nano-beam is demonstrated using the proposed control scheme. For numerical simulation, the parameters of the nano-beam are $\alpha = \beta = 0.1$; consequently, the exact value of the parameters that appeared in (38) is obtained as $K_1 = 97.4$, $K_2 = -19.97$, and $b = 1.09$ [15].

The paper discussed the impact of using nonlocal parameters in modeling a system. Despite this, there may still be uncertainties present that make it necessary to use a disturbance observer. To address this, the proposed controller is specifically designed to work in conjunction with a powerful disturbance observer and reject the effects of all uncertainties. This allows for more accurate modeling and control of the system, despite any remaining uncertainties. Therefore, to better investigate real conditions for the nano-systems, we consider the external disturbance as:

$$d(t) = 0.2 \sin(0.3\pi t) + 0.3 \sin(0.2\pi t) + 0.15 \sin(0.2\sqrt{t+1}) \quad (65)$$

The physical mechanisms of unexpected disturbances and faults in a nano-beam are varied and multifaceted. Some of the key factors that can contribute to these disturbances include thermal expansion or contraction, external forces such as mechanical stress, material defects, control actuator failure, and manufacturing errors.

Thermal expansion or contraction can cause the nano-beam to bend or deform in unexpected ways, leading to unexpected disturbances or faults. Similarly, external forces such as mechanical stress can cause the nano-beam to bend or deform, leading to unexpected disturbances or faults. Material defects such as cracks, voids, or impurities can weaken the nano-beam and make it more susceptible to unexpected disturbances or faults.

Control actuator failure can also cause unexpected disturbances or faults in a nano-beam, as the actuators may not work as intended and thus not provide the expected control on the nano-beam. Manufacturing errors such as improper alignment or uneven distribution of materials can also cause unexpected disturbances or faults in a nano-beam.

It is important to note that these disturbances and faults can be caused by a combination of multiple factors, and not all disturbances or faults are predictable. Therefore, the present research investigates the utilization of the non-local strain gradient theory and a novel fault-tolerant terminal sliding mode control technique to effectively address these disturbances and faults in the stabilization and control of an uncertain Euler–Bernoulli nano-beam with fixed ends.

The user-defined parameter of the control scheme is considered to be:

$$\begin{aligned} k &= 30, \beta = 300, \varepsilon = 55, p_0 = 1, q_0 = 7 \\ \alpha_1 &= 5, \beta_1 = 0.1, \delta = 5, \mu = 1.1, p_1 = 3, q_1 = 7, p_2 = 1, q_2 = 3 \end{aligned} \quad (66)$$

The control gains in the proposed control technique are selected through a process of trial and error. This process involves adjusting the control gains and evaluating the system's performance until the desired level of performance is achieved.

The performance of the proposed control technique has been compared with a PID controller in order to demonstrate its advantages. The control gain of PID is chosen as $K_p = 10$, $K_i = 0.1$, and $K_d = 15$. In this case, we do not consider faults and failures in the actuators, and only the system is analyzed in the presence of external disturbances. The controller is turned on at $t = 2$. Figures 3 and 4 show the results of the stabilization of the nano-beam based on the proposed control technique and the PID controller. As can be seen in these figures, the proposed robust adaptive controller outperforms the PID controller. Additionally, Figure 5 illustrates the excellent performance of the proposed disturbance observer, demonstrating its ability to effectively counteract disturbances and reject them entirely.

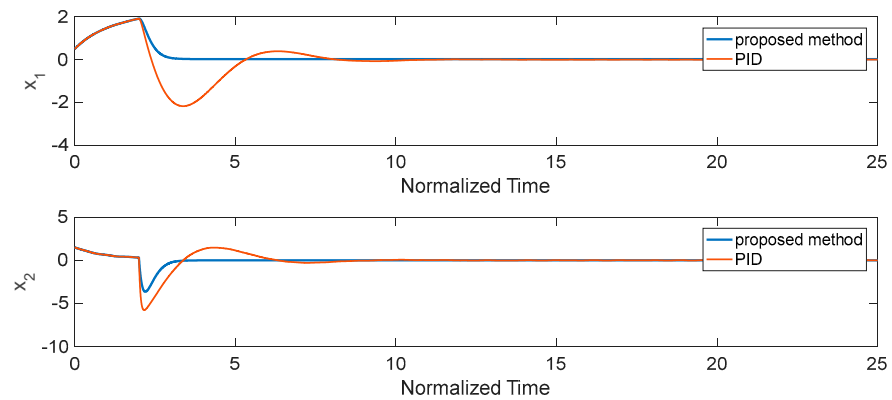


Figure 3. Time history of states of the system based on the proposed method and PID controller.

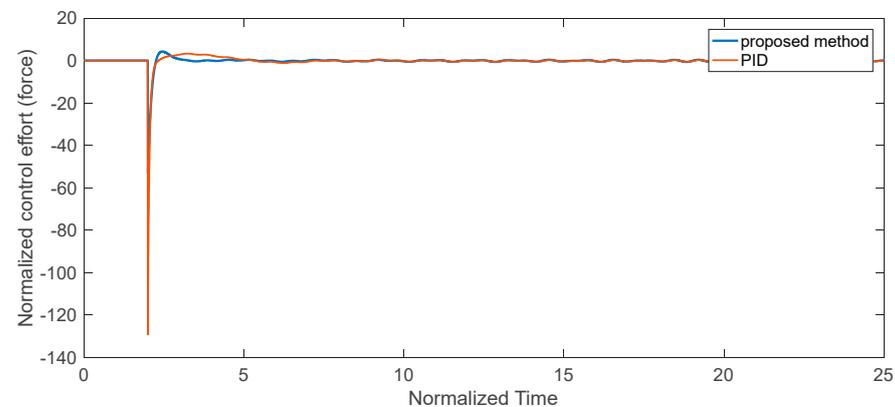


Figure 4. Control input based on the proposed method and PID.

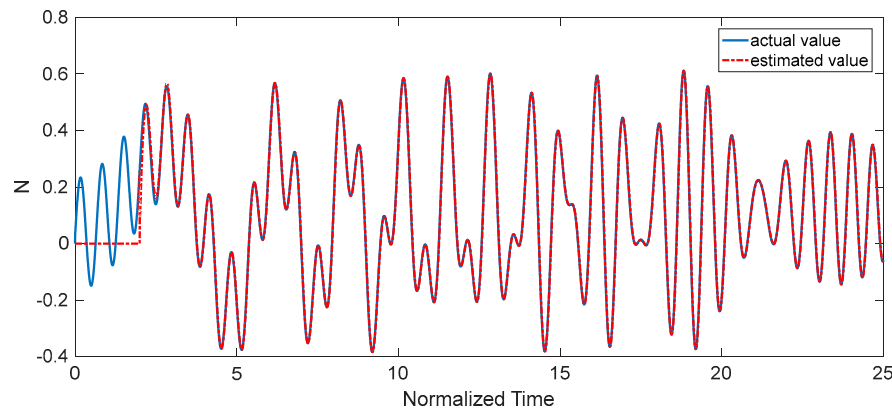


Figure 5. Results of the proposed estimator.

Now, we considered the nano-beam in the presence of faults and failure in the actuator. To this end, in addition to disturbances, the following faults and failure are considered for numerical simulations:

$$\begin{aligned}
 u &= u_c + b(t)((e_i - 1)u_c + \bar{u}) \\
 b(t) &= \begin{cases} 0, & t < t_0 \\ 1 - e^{-a_i(t-t_0)}, & t \geq t_0 \end{cases} \\
 e_i &= 0.7, \quad a_i = 10; \quad t_0 = 10; \quad \bar{u} = 3;
 \end{aligned} \tag{67}$$

Figures 6–9 present the results of stabilizing the nano-beam using the proposed control technique in the presence of disturbances and faults. The controller is turned on at $t = 2$. Figure 6 demonstrates the time history of the deflection of nano-beam based on the proposed control scheme. Based on this figure, after one time unit, the nano-beam is completely

stabilized. Figure 7 demonstrates the time history of deflection of the nano-beam using the proposed control scheme. As is shown in these figures, the proposed controller, which is equipped with the fast estimator, could appropriately deal with uncertainties and faults in the actuator which is an important concern in the control nano-systems. Figure 8 illustrates the performance of the controller in stabilizing the system. In addition, the performance of the estimator is depicted in Figure 9. These results conspicuously confirm that by applying the suggested controller, the states of the system reach their desired values in a short period of time.

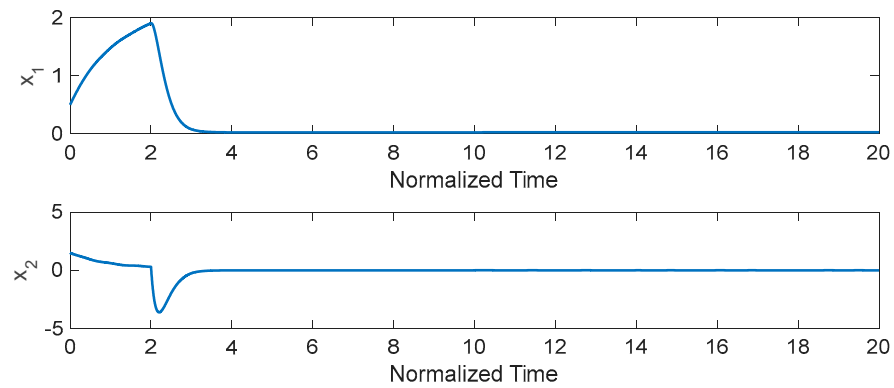


Figure 6. Results of the vibration suppression based on the proposed method in the presence of disturbances and faults in the actuator.

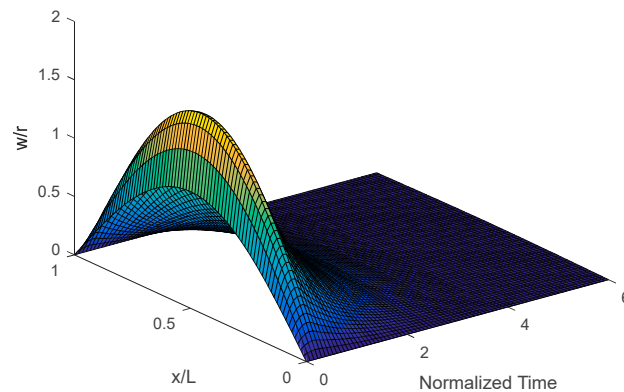


Figure 7. Time history of deflection of the nano-beam using the proposed control scheme in the presence of disturbances and faults in the actuator.

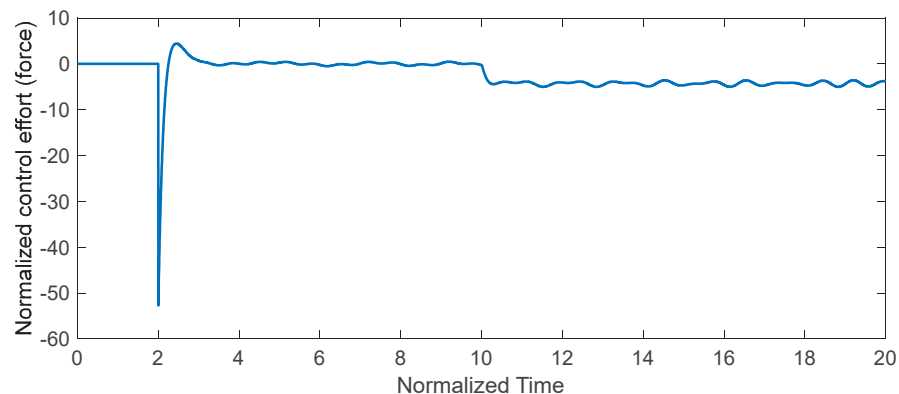


Figure 8. Control command based on the proposed control technique in the presence of disturbances and faults in the actuator.

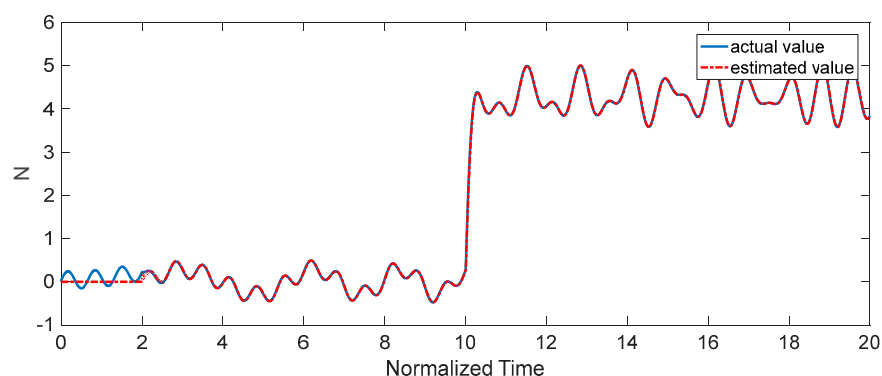


Figure 9. Results of the proposed finite time estimator in the presence of disturbances and faults in the actuator.

In summary, the numerical simulations vividly illustrate the effectiveness of the proposed control scheme for stabilization of the nano-beam when there exist unexpected disturbances and faults.

5. Conclusions

This study examined the stabilization of nonlinear vibrations in nano-beams using the non-local strain gradient theory. The equations of motion for the system were obtained and reduced to an ordinary differential equation using the Galerkin approach. A new disturbance-observer-based fault-tolerant terminal sliding mode control was then developed to stabilize the system, with a disturbance estimator included to handle uncertainties and faults in the control actuator. The stability of the closed-loop system was demonstrated using the Lyapunov stability theorem, and the performance of the proposed control scheme was compared to that of a PID controller through numerical simulations for two different cases. The results showed that the proposed control scheme was effective in stabilizing the uncertain nano-beam. It is acknowledged that terminal sliding mode control is known to have a singularity problem, where the control signal approaches infinity as the sliding surface approaches zero. This singularity problem is a well-known issue in the field of terminal sliding mode control and it is important to consider it. Therefore, it is suggested that some future studies in this field investigate and address the singularity problem in terminal sliding mode control for the control of nano-beams, such as the use of nonsingular sliding surfaces. In addition, future work could involve enhancing its performance using an intelligent fuzzy tuning approach.

Author Contributions: Conceptualization, H.A., A.Y., A.A., N.D.A. and H.J.; Methodology, H.A., A.Y., A.A., N.D.A. and H.J.; Software, H.A., A.Y., A.A., N.D.A. and H.J.; Validation, H.A., A.Y., A.A., N.D.A. and H.J.; Formal analysis, H.A., A.Y., A.A., N.D.A. and H.J.; Investigation, H.A., A.Y., A.A., N.D.A. and H.J.; Resources, H.A., A.Y., A.A., N.D.A. and H.J.; Data curation, H.A., A.Y., A.A., N.D.A. and H.J.; Writing—original draft, H.A., A.Y., A.A., N.D.A. and H.J.; Writing—review & editing, H.A., A.Y., A.A., N.D.A. and H.J.; Visualization, H.A., A.Y., A.A., N.D.A. and H.J.; Supervision, H.A., A.Y., A.A., N.D.A. and H.J.; Project administration, H.A., A.Y., A.A., N.D.A. and H.J.; Funding acquisition, H.A., A.Y., A.A., N.D.A. and H.J. All authors have read and agreed to the published version of the manuscript.

Funding: This research work was funded by Institutional Fund Projects under grant no. (IFPIP: 81-135-1443). The authors gratefully acknowledge technical and financial support provided by the Ministry of Education and King Abdulaziz University, DSR, Jeddah, Saudi Arabia.

Data Availability Statement: No new data were created or analyzed in this study. Data sharing is not applicable to this article.

Acknowledgments: This research work was funded by Institutional Fund Projects under grant no. (IFPIP: 81-135-1443). The authors gratefully acknowledge technical and financial support provided by the Ministry of Education and King Abdulaziz University, DSR, Jeddah, Saudi Arabia.

Conflicts of Interest: The authors declare no conflict of interest.

References

1. Djurić, Z.; Jokić, I.; Peleš, A. Fluctuations of the number of adsorbed molecules due to adsorption–desorption processes coupled with mass transfer and surface diffusion in bio/chemical MEMS sensors. *Microelectron. Eng.* **2014**, *124*, 81–85. [[CrossRef](#)]
2. Fitzgerald, P.L.; Parthasarathy, S.; Salcedo, J.A. *Protection Schemes for MEMS Switch Devices*; Google Patents: Alexandria, VA, USA, 2020.
3. Song, J.; Zhou, Y.; Padture, N.P.; Huey, B.D. Anomalous 3D nanoscale photoconduction in hybrid perovskite semiconductors revealed by tomographic atomic force microscopy. *Nat. Commun.* **2020**, *11*, 3308. [[CrossRef](#)]
4. Chen, S.-H.; Michael, A.; Kwok, C.Y. E-beam evaporated polysilicon for lead zirconate titanate-based micro-actuators. *IEEE Electron Device Lett.* **2016**, *37*, 1347–1350. [[CrossRef](#)]
5. Alcheikh, N.; Ouakad, H.M.; Younis, M.I. Dynamics of V-Shaped Electrothermal MEMS-Based Resonators. *J. Microelectromech. Syst.* **2020**, *29*, 1372–1381. [[CrossRef](#)]
6. Lun, F.Y.; Zhang, P.; Gao, F.B.; Jia, H.G. Design and fabrication of micro-optomechanical vibration sensor. *Microfabr. Technol.* **2006**, *120*, 61–64.
7. Cheng, H.M.; Ewe, M.T.S.; Chiu, G.T.C.; Bashir, R. Modeling and control of piezoelectric cantilever beam micro-mirror and micro-laser arrays to reduce image banding in electrophotographic processes. *J. Micromech. Microeng.* **2001**, *11*, 487. [[CrossRef](#)]
8. Aksyuk, V.A.; Pardo, F.; Bolle, C.A.; Arney, S.; Giles, C.R.; Bishop, D.J. Lucent Microstar micromirror array technology for large optical crossconnects. In *MOEMS and Miniaturized Systems*; SPIE: Bellingham, WA, USA, 2000; pp. 320–324.
9. Eltahir, M.A.; Hamed, M.A.; Sadoun, A.M.; Mansour, A. Mechanical analysis of higher order gradient nanobeams. *Appl. Math. Comput.* **2014**, *229*, 260–272. [[CrossRef](#)]
10. Ebrahimi, F.; Salari, E. Size-dependent free flexural vibrational behavior of functionally graded nanobeams using semi-analytical differential transform method. *Compos. Part B Eng.* **2015**, *79*, 156–169. [[CrossRef](#)]
11. Barretta, R.; Faghidian, S.A.; Marotti de Sciarra, F.; Vaccaro, M.S. Nonlocal strain gradient torsion of elastic beams: Variational formulation and constitutive boundary conditions. *Arch. Appl. Mech.* **2020**, *90*, 691–706. [[CrossRef](#)]
12. Yasbolaghi, R.; Khoei, A.R. A continuum–atomistic multi-scale analysis of temperature field problems and its application in phononic nano-structures. *Finite Elem. Anal. Des.* **2022**, *198*, 103643. [[CrossRef](#)]
13. Maugin, G.A. *Non-Classical Continuum Mechanics*; Springer: Berlin/Heidelberg, Germany, 2017.
14. Romanoff, J.; Karttunen, A.T.; Varsta, P.; Remes, H.; Reinaldo Goncalves, B. A review on non-classical continuum mechanics with applications in marine engineering. *Mech. Adv. Mater. Struct.* **2020**, *27*, 1065–1075. [[CrossRef](#)]
15. Şimşek, M. Nonlinear free vibration of a functionally graded nanobeam using nonlocal strain gradient theory and a novel Hamiltonian approach. *Int. J. Eng. Sci.* **2016**, *105*, 12–27. [[CrossRef](#)]
16. Yang, F.; Chong, A.C.M.; Lam, D.C.C.; Tong, P. Couple stress based strain gradient theory for elasticity. *Int. J. Solids Struct.* **2002**, *39*, 2731–2743. [[CrossRef](#)]
17. Mindlin, R.D.; Tiersten, H.F. *Effects of Couple-Stresses in Linear Elasticity*; Columbia Univ.: New York, NY, USA, 1962.
18. Mindlin, R.D. Second gradient of strain and surface-tension in linear elasticity. *Int. J. Solids Struct.* **1965**, *1*, 417–438. [[CrossRef](#)]
19. Fleck, N.A.; Hutchinson, J.W. A phenomenological theory for strain gradient effects in plasticity. *J. Mech. Phys. Solids* **1993**, *41*, 1825–1857. [[CrossRef](#)]
20. Lam, D.C.C.; Yang, F.; Chong, A.C.M.; Wang, J.; Tong, P. Experiments and theory in strain gradient elasticity. *J. Mech. Phys. Solids* **2003**, *51*, 1477–1508. [[CrossRef](#)]
21. Eringen, A.C. Nonlocal polar elastic continua. *Int. J. Eng. Sci.* **1972**, *10*, 1–16. [[CrossRef](#)]
22. Aifantis, E.C. On the role of gradients in the localization of deformation and fracture. *Int. J. Eng. Sci.* **1992**, *30*, 1279–1299. [[CrossRef](#)]
23. Lim, C.W.; Zhang, G.; Reddy, J.N. A higher-order nonlocal elasticity and strain gradient theory and its applications in wave propagation. *J. Mech. Phys. Solids* **2015**, *78*, 298–313. [[CrossRef](#)]
24. Tajaddodianfar, F.; Pishkenari, H.N.; Yazdi, M.R.H.; Miandoab, E.M. Size-dependent bistability of an electrostatically actuated arch NEMS based on strain gradient theory. *J. Phys. D Appl. Phys.* **2015**, *48*, 245503. [[CrossRef](#)]
25. Rahmani, O.; Pedram, O. Analysis and modeling the size effect on vibration of functionally graded nanobeams based on nonlocal Timoshenko beam theory. *Int. J. Eng. Sci.* **2014**, *77*, 55–70. [[CrossRef](#)]
26. Jahanshahi, H.; Yousefpour, A.; Munoz-Pacheco, J.M.; Moroz, I.; Wei, Z.; Castillo, O. A new multi-stable fractional-order four-dimensional system with self-excited and hidden chaotic attractors: Dynamic analysis and adaptive synchronization using a novel fuzzy adaptive sliding mode control method. *Appl. Soft Comput.* **2020**, *87*, 105943. [[CrossRef](#)]
27. Jahanshahi, H.; Rajagopal, K.; Akgul, A.; Sari, N.N.; Namazi, H.; Jafari, S. Complete analysis and engineering applications of a megastable nonlinear oscillator. *Int. J. Non-Linear Mech.* **2018**, *107*, 126–136. [[CrossRef](#)]
28. Yao, Q.; Jahanshahi, H.; Bekiros, S.; Mihalache, S.F.; Alotaibi, N.D. Gain-Scheduled Sliding-Mode-Type Iterative Learning Control Design for Mechanical Systems. *Mathematics* **2022**, *10*, 3005. [[CrossRef](#)]
29. Yao, Q.; Jahanshahi, H.; Moroz, I.; Bekiros, S.; Alassafi, M.O. Indirect neural-based finite-time integral sliding mode control for trajectory tracking guidance of Mars entry vehicle. *Adv. Space Res.* **2022**; *in press*.

30. Yousefpour, A.; Jahanshahi, H.; Munoz-Pacheco, J.M.; Bekiros, S.; Wei, Z. A fractional-order hyper-chaotic economic system with transient chaos. *Chaos Solitons Fractals* **2020**, *130*, 109400. [[CrossRef](#)]
31. Jahanshahi, H.; Yousefpour, A.; Wei, Z.; Alcaraz, R.; Bekiros, S. A financial hyperchaotic system with coexisting attractors: Dynamic investigation, entropy analysis, control and synchronization. *Chaos Solitons Fractals* **2019**, *126*, 66–77. [[CrossRef](#)]
32. Yousefpour, A.; Haji Hosseinloo, A.; Reza Hairi Yazdi, M.; Bahrami, A. Disturbance observer-based terminal sliding mode control for effective performance of a nonlinear vibration energy harvester. *J. Intell. Mater. Syst. Struct.* **2020**, *31*, 1495–1510. [[CrossRef](#)]
33. Jahanshahi, H.; Yousefpour, A.; Munoz-Pacheco, J.M.; Kacar, S.; Pham, V.T.; Alsaadi, F.E. A new fractional-order hyperchaotic memristor oscillator: Dynamic analysis, robust adaptive synchronization, and its application to voice encryption. *Appl. Math. Comput.* **2020**, *383*, 125310. [[CrossRef](#)]
34. Yang, Q.; Ge, S.S.; Sun, Y. Adaptive actuator fault tolerant control for uncertain nonlinear systems with multiple actuators. *Automatica* **2015**, *60*, 92–99. [[CrossRef](#)]
35. Haghparast, M.; Navi, K. Design of a novel fault tolerant reversible full adder for nanotechnology based systems. *World Appl. Sci. J.* **2008**, *3*, 114–118.
36. Rhoads, J.F.; Shaw, S.W.; Turner, K.L. The nonlinear response of resonant microbeam systems with purely-parametric electrostatic actuation. *J. Micromech. Microeng.* **2006**, *16*, 890. [[CrossRef](#)]
37. Jin, X. Fault tolerant finite-time leader–follower formation control for autonomous surface vessels with LOS range and angle constraints. *Automatica* **2016**, *68*, 228–236. [[CrossRef](#)]
38. Zuo, Z.; Ho, D.W.C.; Wang, Y. Fault tolerant control for singular systems with actuator saturation and nonlinear perturbation. *Automatica* **2010**, *46*, 569–576. [[CrossRef](#)]
39. Murugesan, S.; Goel, P.S. Fault-tolerant spacecraft attitude control system. *Sadhana* **1987**, *11*, 233–261. [[CrossRef](#)]
40. Zhihong, M.; Yu, X.H. Terminal sliding mode control of MIMO linear systems. *IEEE Trans. Circuits Syst. I Fundam. Theory Appl.* **1997**, *44*, 1065–1070. [[CrossRef](#)]

Disclaimer/Publisher’s Note: The statements, opinions and data contained in all publications are solely those of the individual author(s) and contributor(s) and not of MDPI and/or the editor(s). MDPI and/or the editor(s) disclaim responsibility for any injury to people or property resulting from any ideas, methods, instructions or products referred to in the content.